JOURNAL OF MATERIALS SCIENCE 32 (1997) 6015–6019

Crystallization of amorphous $Fe_{73.5}Si_{13.5}B_9Nb_3Cu_1$

F. BRANDA*, A. COSTANTINI*, L. LANOTTE**
** Dipartimento di Ingegneria dei Materiali e della Produzione, and ** Dipartimento di Scienze Fisiche, Unità CINFM, Piazzale Tecchio 80125 Napoli, Italy*

P. MATTEAZZI
Istituto di Chimica, Facoltà di Ingegneria, Via Cotonificio 108, 44133 Udine, Italy

A study is reported on the devitrification behaviour of the amorphous alloy $Fe_{73.5}Si_{13.5}B_9Nb_3Cu_1$. Samples of the studied glass underwent isothermal and non-isothermal heat treatments in a thermal analysis apparatus. In addition some samples were very rapidly heated to very high temperatures by means of a laser beam. In this way a large temperature range was explored and information was obtained on the overall thermal evolution of the studied amorphous alloy. The experimental results suggest that, as recently proposed in the literature, nanocrystallization can be linked to a rate limiting Nb diffusion stage in the crystal growth process. However topological short range ordering (TSRO) and chemical short range ordering (CSRO) also affect the devitrification behaviour. In the case of the studied alloy, three temperature ranges can be defined. At low temperature only TSRO occurs. Above a temperature that lies approximately in the range 450–500 °C, glass in glass phase separation occurs up to a temperature that lies approximately in the range 700–750 °C, above which it appears to be very limited. The occurrence of glass in glass phase separation appears to be necessary to obtain a fine microstructure, because Nb concentrates in the boron depleted, iron rich glassy phase. The occurrence of TSRO prior to demixing should be avoided if nanocrystallization is desired. All this appears to be satisfied by isothermally treating the sample at a temperature of 555 °C.

1. Introduction

Amorphous alloys between transition metals and the metalloid elements B, P and Si, are relatively easy to quench from the melt and have mechanical and magnetic properties sufficiently remarkable to warrant commercial exploitation. Among the most prominent examples are the iron based FeSiBNbCu alloys whose crystallization can give nanocrystalline structures which offer a new opportunity for "tailoring" soft magnetic properties [1]. Many studies of their magnetic [1–5], magnetoelastic [6–8] and electrical properties [9] have been reported.

In this paper a study of the devitrification behaviour of an amorphous alloy with the composition $Fe_{73.5}Si_{13.5}B_9Nb_3Cu_1$ is reported. Samples of the studied glass were submitted to isothermal and non-isothermal heat treatment in a thermal analysis (TA) apparatus. In addition some samples were very rapidly heated to very high temperatures by means of a laser beam. In this manner a large temperature range was explored and information on the overall thermal evolution of the studied amorphous alloy was obtained.

2. Experimental procedures

The ~16 μm thick amorphous ribbons used in this investigation were prepared by rapid quenching from the melt (single roller technique, average velocity of 35 m s^{-1}), at the Italian national electrotechnical institute "G. Ferraris" and kindly supplied to us for these experiments. The samples for the different heat treatments were all cut from the same ribbon.

Thermal analysis (TA) was performed using a Netzsch differential scanning calorimeter (DSC) heat flux model 404M on about 5 mg samples at various heating rates (5–80 °C min^{-1}) in an inert atmosphere. Powdered Al_2O_3 was used as a reference material.

Isothermal heating was carried out in a furnace with a close control of the temperature; when the planned temperature was reached and stabilized, a small cell, containing the sample, was inserted into the furnace. A static helium atmosphere was maintained in the cell during the heat treatment. When the allowed time had elapsed, the cell was taken out from the furnace and the sample was cooled, in about 2 min, to room temperature in a stream of helium.

Laser annealing was performed by means of a well established technique [10, 11]. The samples were irradiated with a CO_2 laser beam defocused to a spot diameter of 40 mm, in order to obtain uniform heating. A helium jet was used to rapidly cool the sample to room temperature after the irradiation. The samples were passed orthogonal to the laser beam, whose power was maintained constant, at a constant velocity

0022–2461

of 2.8 cm s^{-1}. Six samples were laser annealed at different laser powers in the range of 20–50 W. The heating curves for the six laser beam powers selected are shown in Fig. 1. They were obtained using a well characterized model [12, 13].

X-ray diffraction (XRD) patterns were recorded using Co-K_α radiation on a INEL diffractometer equipped with a PSD 120 counter. The crystallite size was calculated from the full width at half maximum of the X-ray peaks, taking into account both the instrumental broadening and internal strain effects [14, 15]. In the case of partially devitrified samples, the deconvolution of XRD reflections allowed the evaluation of the devitrified volume fraction.

3. Results

In Fig. 2 a TA curve is reported, recorded at a heating rate $\beta = 20\,^{\circ}C\,min^{-1}$, relative to an as quenched sample. As can be seen two exothermic-peaks are clearly visible. When the heating rate is varied between 5 to 80 °C min^{-1}, the temperature of the first peak changes in the range 525–570 °C, while the second one occurs in the range 660–710 °C. The ratio of the areas of the second to first peak appears to be dependent on the heating rate. In Fig. 3 the ratio, *R*, of the areas is reported as a function of the heating rate, β. Taking into account that the peak area is proportional to the heat evolved [16], as long as the ratio of the molar heat of crystallization can be considered constant, the ratio *R* can be interpreted as the ratio of crystallized amounts. It is remarkable that the curve of *R* as a function of β shows a maximum. Some samples were heated at a constant heating rate, β, of 2 °C min^{-1}, up to 410, 450 and 490 °C, that is in the temperature range where the TA curve does not show any exothermic effect, and afterwards were submitted to a TA run at $\beta = 20\,^{\circ}C\,min^{-1}$. The TA curves are very similar to the one reported in Fig. 2. No influence of the pretreatment was observed on the peak temperatures; however, as is shown in Fig. 3, the ratio of the second to first peaks progressively lowers as the end temperature of the pretreatment is raised.

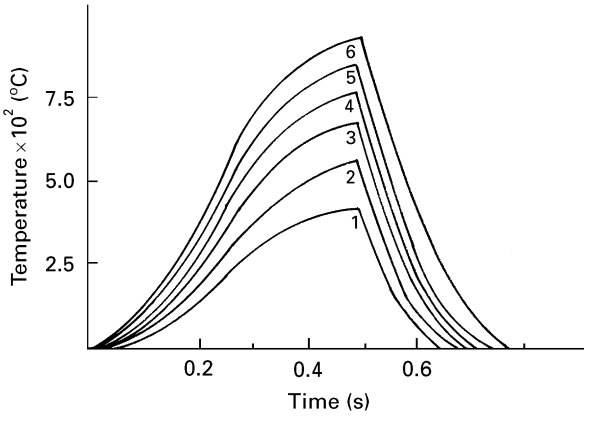

Figure 1 Laser annealing heating curves relative to different incident laser powers: (1) 24 W; (2) 32 W; (3) 38 W; (4) 42 W; (5) 45 W and (6) 50 W.

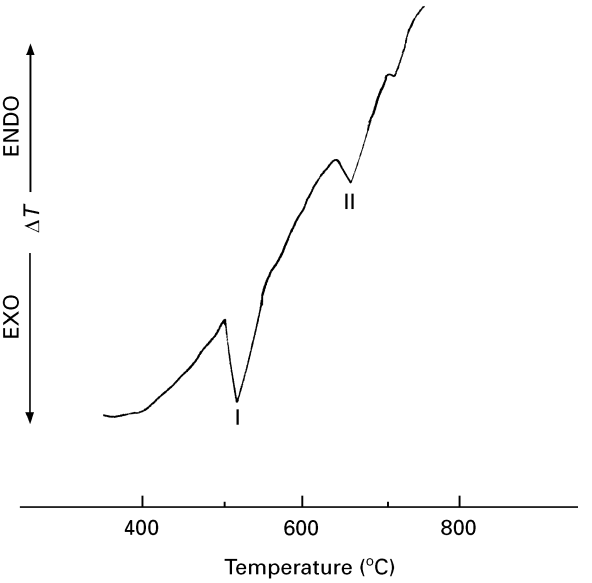

Figure 2 A typical TA run.

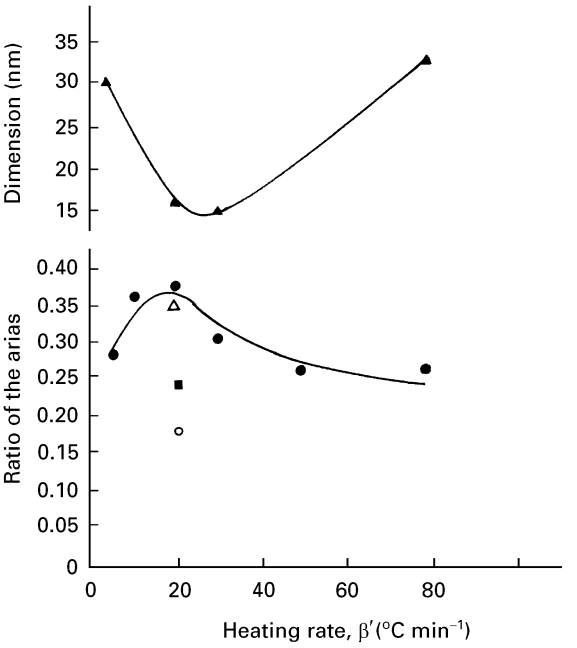

Figure 3 Ratio, *R*, of the areas of the II to I TA exothermic-peaks as a function of the heating rate for as quenched samples (●) and samples previously submitted to a slow TA run at 2 °C min^{-1} up to 410 °C (△), 450 °C (○), and 490 °C (■). The dimensions of the iron based solid solution crystals formed during the TA run are also reported (▲).

Devitrified samples were submitted to XRD analysis, and some of the collected patterns are shown in Fig. 4. Some samples were isothermally heat treated for 5 min at 555 and 695 °C, that is in the temperature range of the first and second DTA exothermic-peaks; and at a temperature a little above, 750 °C. Diffraction pattern (d) in Fig. 4 is of a sample submitted to a TA run stopped at the peak temperature of the second exothermic effect, which is qualitatively representative of all the samples devitrified during a TA run. As can be seen reflections of αFe, in which silicon dissolves, and of iron boride occur in the XRD patterns of the samples treated at 550 and 690 °C. However in the

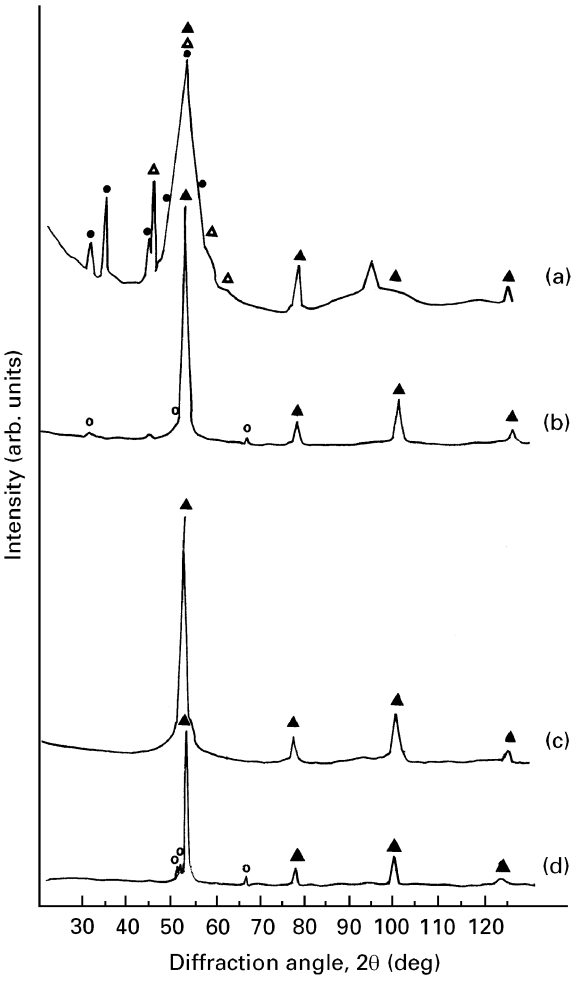

Figure 4 XRD patterns after 5 min at 555 °C (a), 695 °C (b) and 750 °C (c), and after a TA run recorded at 20 °C min^{-1} stopped at the peak temperature of the II exo-effect (d). (▲) Fe based solid solution; (●) Fe_3B; (△) $Fe_{23}B_6$; (○) Fe_2B.

case of the isothermal treatment at 750 °C only the αFe reflections appear. Therefore the first exothermic peak of the DTA curves can be associated with the formation of the iron based solid solution that forms in a greater amount than the iron boride. However the outline of the XRD reflections changes from sample to sample, because of differences in the crystal dimensions. In Fig. 3 the mean dimensions of the crystals of the iron based solid solution formed during the TA run are reported as a function of the heating rate, β. The curve displays a minimum. The dimensions are comparable with those reported by van Bouwelen *et al.* [17] for samples of the very close composition, $Fe_{75.5}Si_{12.5}B_8Nb_3Cu_1$, isothermally treated at 550 °C. In Fig. 5 the mean dimensions of the crystals formed during the isothermal heat treatments are reported as a function of the temperature.

Some samples were submitted to laser annealing. When a laser beam is used, it is possible to heat at very high heating rate making the sample reach very high temperatures without crystallizing. Six samples were submitted to the laser annealing cycles indicated in Fig. 1. Devitrification always occurred to some extent, except for the case of heating cycle 1, in which the sample remained amorphous. The XRD patterns relative to devitrified samples are all similar to the one reported in pattern (c) of Fig. 4, that is only the iron based solid solution was detected. In Fig. 6 the degree of crystallinity and the mean dimension of the crystals formed, evaluated from the XRD patterns, are reported as a function of the maximum temperature reached during the laser annealing cycle. Some samples were successively submitted to a TA run at a heating rate of $\beta = 20\,^{\circ}C\,min^{-1}$. The thus devitrified samples were submitted to XRD analysis; the recorded patterns are similar to the one reported as pattern (d) in Fig. 4, that is both the iron based solid solution and the iron boride were present after the TA run. Moreover the TA curves are similar to the one reported in Fig. 2, showing the presence of two exothermic-peaks. However the ratio of the second to first peak areas changes, with the laser annealing cycle. This ratio has been corrected to take into account the point that the laser annealed samples were already somewhat devitrified. Therefore the area of the first

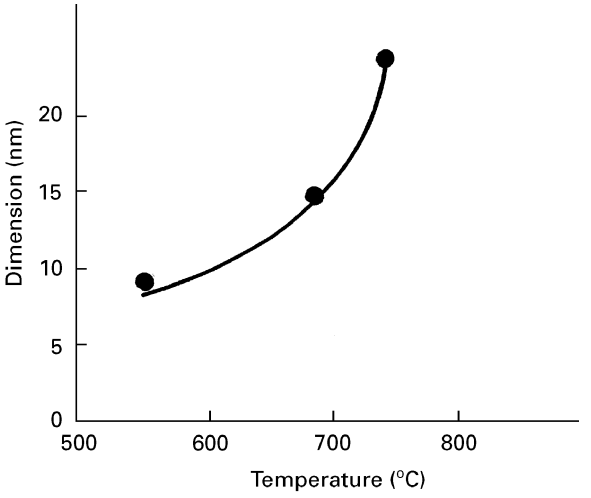

Figure 5 Dimension of the crystals formed after 5 min of isothermal heat treatment, as a function of the temperature.

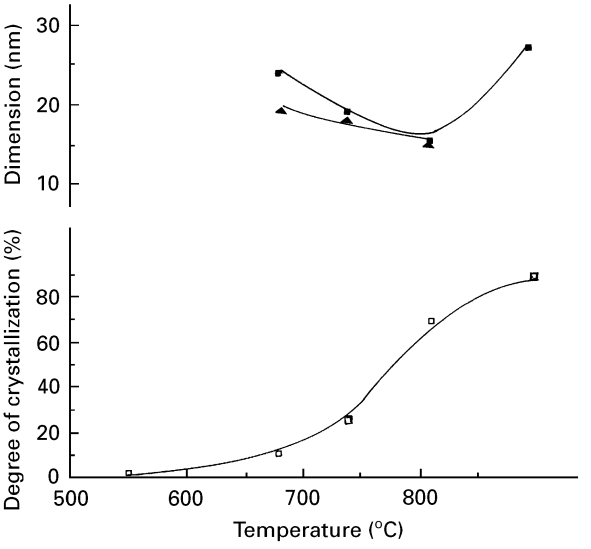

Figure 6 Crystallization degree (□) and dimensions of crystals of the iron based solid solution (■) formed during laser annealing as a function of the maximum temperature reached. (▲) Crystal dimensions of the same phase when the laser annealed samples are submitted to a TA run at 20 °C min^{-1}.

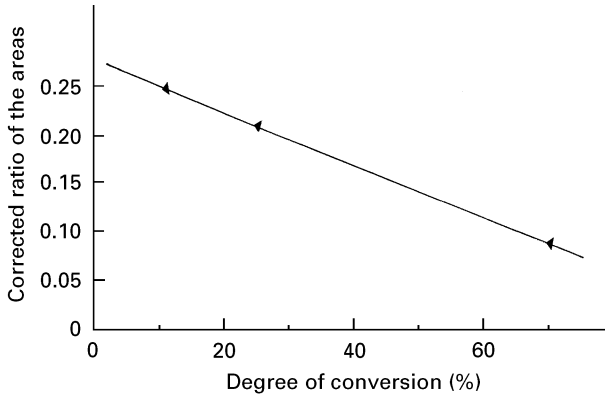

Figure 7 Corrected ratio, R_c, (as defined in the text), of the areas of the II to I TA exothermic-peaks relative to laser annealed samples.

peak was increased on the basis of the results reported in Fig. 6, to take into account the amount of the iron based solid solution formed during laser annealing. This corrected ratio, R_c, has the meaning of the ratio of the overall devitrified amounts of the two phases and has been plotted against the crystallization degree obtained during the laser annealing. Fig. 7 shows that this corrected ratio, R_c, decreases as the crystallinity degree, obtained at the higher temperature produced by laser annealing, increases.

4. Discussion

When an amorphous alloy is annealed, there may be several kinds of topological short range ordering (TSRO) in the structure and chemical short range ordering (CSRO) [18–20]. The CSRO can give rise, in off-stoichiometric amorphous alloys, to a demixing effect. When metastable immiscibility occurs a consolute temperature is defined above which no demixing occurs. Below this temperature the composition and relative amounts of the glass in glass separated phases depends on the temperature and on the nominal composition of the alloy [21]. The results of Fig. 2 can be easily explained if it is admitted that CSRO occurs in the studied system giving rise to a boron rich phase and a boron depleted one. In the comments to Fig. 3, in the previous section, the changes in R have been interpreted as changes in the crystallized amounts of the two phases. These could be the consequence of a variation of the amounts of the boron rich separated phase.

It is known, that the effect of increasing the TA heating rate is to shift all the transformations towards higher temperatures. Taking into account that kinetics increase as the temperature is raised, the trend of the curve in Fig. 3 can be justified if one, also, admits that the immiscibility dome and the composition studied are such that the amount of the separated boron rich phase decreases as the temperature increases. The presence of a maximum in the curve of Fig. 3 may, thus, be the result of a compromise between thermodynamic and kinetic factors. The latter could be expected to have a particularly severe effect if we consider that TSRO, that involves very limited movements, is active at all temperatures. In particular, the occurence of TSRO in a sample heat treated at low temperature where no long range diffusion easily occurs (and, therefore, glass in glass phase separation and devitrification are kinetically hindered) should kinetically hinder the glass in glass phase separation at a higher temperature.

In this connection there are several other clues; firstly, as shown by Fig. 4, iron boride does not form during isothermal heat treatments at 750 °C. This result confirms the existence of a consolute temperature which should be lower than 750 °C. Secondly, it is useful to consider the progressive fall, observed in Fig. 3, of the ratio of the second to first peak areas when the TA is performed at 20 °C min^{-1} on samples previously heat treated at a lower heating rate (2 °C min^{-1}) up to 410, 450 or 490 °C. One can speculate that the extensive annealing at lower temperatures, where only TSRO would occur, limits the glass in glass phase separation, that would occur prevalently at higher temperatures in the subsequent TA run.

Moreover the results involving the laser annealing can be easily explained. It can be estimated, from Fig. 1, that, when the laser power is changed, the mean values of the heating rate change from $\sim 50\,000$ to $\sim 100\,000$ °C min^{-1}. Therefore all the transformations are forced to occur in a temperature range higher than in a TA cycle. In particular in the case of the laser annealing treatments 3–6 of Fig. 1, where the maximum temperature reached varies between 680 to 900 °C, the transformations occur at temperatures that bear little relation to these explored during the TA experiments. It's useful to observe that, as is shown in Fig. 4, during the laser annealing only the iron based solid solution is formed; in particular, when the highest temperature is reached (treatment 6 of Fig. 1), a 90% crystallization degree is detected, as shown in Fig. 6. Since the boron content is 9 wt % it is probable that in this case almost all the Fe and Si form the iron based solid solution and thus glass in glass phase separation would not occur at all. In the other cases, however, when the laser annealed samples are submitted to TA, Fig. 7 shows that the "corrected ratio", R_c, of the second to first peak area progressively lowers as the cristallinity percentage obtained during the laser annealing is increased. All this suggests that the laser annealing treatments 3–6 rapidly expose the samples to temperatures at which phase separation is very limited or does not occur at all. Demixing would therefore occur during the subsequent TA run in a glassy phase in which the iron concentration available for the phase separation is lower the higher the crystallinity percentage obtained during the laser annealing. The results of Fig. 7 would be, therefore, justified.

Fig. 6 shows that, as the devitrification temperature range is raised, although greater crystallinity percentages are obtained, the mean dimension of the crystals passes through a minimum. Another minimum, however, is found, as shown by Fig. 3, in the case of samples devitrified during a TA run, that is in a lower temperature range. The existence of a minimum, when the heating rate is changed, can be explained by

considering that, as often occurs in the case of metallic glasses, the nucleation and crystal growth curves are superimposed. In fact when the curves are well separated, as in the case of silicate glasses, the increase of the heating rate reduces the time spent in the temperature range of efficient nucleation. Therefore a continuous increase in the crystal dimensions would be expected as the result of the lower number of nuclei formed [22, 23]. However the presence of two minima requires an explanation. In fact the smallest dimension is expected at the temperature at which the nucleation rate is maximum. It is worth noting that, recently, it was proposed that Nb played an important role in the devitrification of an amorphous alloy with a composition of $Fe_{75.5}Si_{12.5}B_8Nb_3Cu_1$ [17] that is close to that of the material studied in this paper. In particular nanocrystallization could be linked to a rate limiting Nb diffusion stage in the crystal growth process, which would hinder the growth of larger crystals. When the fraction of crystalline material increases, especially around relatively large crystals, the amorphous phase becomes richer in Nb which makes the crystallization more difficult which favours the growth of smaller crystals.

Therefore the occurrence, in Fig. 3, of a minimum in the crystal dimension at the value of the heating rate for which the ratio R is a maximum, could be the consequence of the increase in the Nb concentration in the boron depleted phase. Also the apparent decrease, shown in Fig. 6, of the crystal dimension when the laser annealed samples are submitted to TA also finds a simple explanation. In fact the Nb is expected to concentrate around the growing crystals. Therefore when devitrification is stopped and forced to continue at a lower temperature, where the Nb diffusion rate is reduced, we must expect that only the smaller crystals formed at lower temperatures can grow and thus the mean crystal dimension must decrease.

Finally the results of Fig. 5 can be explained. The higher the temperature of the isothermal treatment the coarser the microstructure. This can be ascribed to the following two causes: (a) a higher diffusion rate of Nb and (b) reduced glass in glass phase separation. The crystal dimension in the case of the isothermal treatment at 555 °C is lower than the ones obtained during the TA runs, where devitrification occurs in the temperature range 500–600 °C. In tandem with the above discussion, these results should be linked to the fact that if a sample is heated to the temperature range of efficient demixing, by rapidly crossing the one where only TSRO is active, it would be more prone to undergo more extensive glass in glass phase separation and smaller crystals should be formed.

5. Conclusion

The experimental results suggest that, as recently proposed in the literature, Nb plays an important role in the devitrification of the alloy. In particular nanocrystallization can be linked to a rate limiting Nb diffusion stage in the crystal growth process. However TSRO and CSRO also affect the devitrification behaviour. In the case of the studied alloy, three temperature ranges can be defined. At low temperature only TSRO occurs. Above a temperature that lies approximately in the range 450–500 °C, glass in glass phase separation occurs up to a temperature that lies approximately in the range 700–750 °C, above which it appears to be very limited. The occurrence of glass in glass phase separation appears to be necessary to obtain a fine microstructure, because Nb concentrates in the boron depleted, iron rich glassy phase. The occurrence of TSRO prior to demixing should be avoided if nanocrystallization is desired. All this appears to be satisfied by isothermally treating the sample at a temperature of 555 °C.

References

1. G. HERZER, *J. Magn. Magn. Mater.* **112** (1992) 258.
2. T. H. NOH, W. K. PI, H. J. KIM and I. K. KANG, *J. Appl. Phys.* **69** (1991) 5921.
3. P. MATTA, P. SOVAK, M. KONC and T. SVEC, *J. Magn. Magn. Mater.* **140–144** (1995) 329.
4. P. KOLLAR, L. KAFKOVA, J. FUZER and M. KONC, *ibid.* **140–144** (1995) 333.
5. T. KULIK, R. ZUBEREK and A. HERNANDO, *ibid.* **140–144** (1995) 433.
6. E. BONETTI, L. DEL BIANCO and P. TIBERTO, *ibid.* **140–144** (1995) 477.
7. Z. KACZCOWSKI, L. LANOTTE and M. MÜLLER, *ibid.* **140–144** (1995) 325.
8. Z. KACZCOWSKI, L. MALKINSKI and M. MÜLLER, *IEEE Trans. Magn.* **31** (1995) 791.
9. P. ALLIA, M. BARICCO, P. TIBERTO and F. VINAI, *J. Non-Cryst. Solids* **156–158** (1993) 585.
10. L. LANOTTE, P. MATTEAZZI and V. TAGLIAFERRI, *J. Magn. Magn. Mater.* **42** (1984) 183.
11. L. LANOTTE and P. MATTEAZZI, *ibid.* **61** (1986) 225.
12. L. LANOTTE and V. TAGLIAFERRI, *High Temp. Mater. Proc.* **7** (1986) 25.
13. L. LANOTTE, P. SILVESTRINI and V. TAGLIAFERRI, *Il Nuovo Cimento* **13D** (1991) 1123.
14. P. MATTEAZZI and G. LE CAER, *J. Amer. Ceram. Soc.* **75** (1992) 2749.
15. H. P. KLUG and L. E. ALEXANDER, "X-ray diffraction procedures" (Wiley, New York, 1974).
16. S. L. BOERSMA, *J. Amer. Ceram. Soc.* **38** (1955) 281.
17. F. VAN BOUWELEN, J. SIESTMA and A. VAN DEN BEUKEL, *J. Non-Cryst. Solids* **156–158** (1993) 567.
18. P. H. GASKELL, *ibid.* **32** (1979) 207.
19. H. HERMANN and W. KREHER, *J. Phys. F: Met. Phys.* **18** (1988) 641.
20. Z. G. LIU, X. J. WU, Y. CHEN, X. WU and X. Y. QIN, *J. Non-Cryst. Solids* **109** (1989) 262.
21. Z. STRNAD, "Glass–ceramic materials" (Elsevier, Amsterdam, 1986).
22. A. MAROTTA, A. BURI and F. BRANDA, *Thermochim. Acta* **40** (1980) 397.
23. K. MATUSITA and S. SAKKA, *Bull. Int. Chem. Res. Kyoto Univ.* **59** (1981) 159.

Received 3 May 1996
and accepted 28 April 1997